Magnetostructural correlations in the tetranuclear series of $\{Fe_3LnO_2\}$ butterfly core clusters: Magnetic and Mössbauer spectroscopic study

J. Bartolomé,[1] G. Filoti,[2] V. Kuncser,[2] G. Schinteie,[2] V. Mereacre,[3,4] C. E. Anson,[4] A. K. Powell,[4] D. Prodius,[3] and C. Turta[3]

[1]*Instituto de Ciencia de Materiales de Aragón and Departamento de Física Materia Condensada, CSIC–Universidad de Zaragoza, 50009 Zaragoza, Spain*

[2]*National Institute of Physics of Materials, P. O. Box MG 7, 77125 Bucharest-Magurele, Romania*

[3]*Laboratory of Bioinorganic Chemistry, Institute of Chemistry of the Academy of Sciences of Moldova, 3 Academy Str., MD-2028 Chisinau, Moldova*

[4]*Institute of Inorganic Chemistry, University of Karlsruhe, Engesser Str., Grb. 30.45, D-76128 Karlsruhe, Germany*

(Received 8 April 2009; revised manuscript received 4 June 2009; published 27 July 2009)

Six tetranuclear complexes $[Fe(III)_3Ln(\mu_3\text{-}O)_2(CCl_3COO)_8(H_2O)(THF)_3]\cdot THF\cdot C_7H_{16}$ [Ln=Gd(III) (1), Tb(III) (2), Dy(III) (3), Ho(III) (4), Y(III) (5), and Lu(III) (6)] have been studied by magnetic susceptibility and Mössbauer spectroscopy. These isostructural molecules have a "butterfly" structure core consisting of two $Fe_2Ln(\mu_3\text{-}O)$ triangular "wings" which share a common Ln-Fe "body"; the dihedral angle between the wings is ca. 148°. The coordination spheres of the iron ions are essentially distorted octahedral. The lanthanides are eight-coordinate with coordination polyhedra that may be described as distorted tetragonal bipyramids. Variable-temperature solid-state magnetic susceptibility in the temperature range 1.8–300 K and magnetization at 1.8 K for compounds 1–6 were measured. The spin state of Fe is $S=5/2$ in all cases. In compounds 5 and 6, where Ln(III) (Y and Lu, respectively) is diamagnetic, the three Fe atoms form an obtuse isosceles triangle with antiferromagnetic interactions $J_{Fe\text{-}Fe}=-50$ K between the wing-tip Fe_w and body Fe_b atoms, and negligible interaction between the Fe_w's, resulting in a ground state of effective spin $S=5/2$ per cluster. In the complexes with paramagnetic lanthanide ions, the interaction between the Fe_3 triangle and the Ln(III) center is described by an effective exchange constant which is antiferromagnetic and 1 order of magnitude weaker. Besides, at 3 K incipient spin blocking, characteristic of single molecule magnets, was found to occur in the out-of-phase component of the ac susceptibility in $\{Fe_3TbO_2\}$, $\{Fe_3DyO_2\}$, and $\{Fe_3HoO_2\}$. The activation energy of a Debye process describing the magnetization reversal has been determined to be, $E_a\approx 8$, 9, and 10 K for the Ln=Tb, Dy, and Ho, respectively, and the prefactor $\tau_0\approx 10^{-7}$ s. The high spin states of the Fe(III) centers were confirmed by the Mössbauer spectra, in which two distinguishable Fe sites could be resolved above 80 K, corresponding to the Fe_w and Fe_b sites, respectively. Relatively larger values of the quadrupole splitting of the Mössbauer spectra were observed for the Fe_w pair as compared with that for the Fe_b, and both quadrupole splittings diminished with increasing temperature. At 3 K the Mössbauer spectra showed a state with blocked spins (sextets) for the $\{Fe_3TbO_2\}$ and $\{Fe_3DyO_2\}$ cases. From the E_a and τ_0, determined in the ac susceptibility, the relaxation time at 3 K is estimated as $\tau\approx 10^{-5}-10^{-6}$ s much longer than the time window of Mössbauer spectroscopy and compatible with the single molecule magnet behavior. In the presence of a strong magnetic field the moments of the Ln(III) cation and the Fe_3 triangle are polarized. For some compounds at low temperature a magnetic pattern (sextet) for each of the three Fe sites appeared, and the antiferromagnetic coupling within the Fe_3 cluster was directly proved by the opposite trend of the field dependence of the two Fe_w sextets as compared with the Fe_b third one.

DOI: 10.1103/PhysRevB.80.014430 PACS number(s): 75.50.Xx, 71.70.Gm, 73.22.−f, 75.30.Ds

I. INTRODUCTION

At present the synthesis and research on new polynuclear coordination compounds, which possess the properties of single molecule magnets, are of paramount importance.[1–3] Polynuclear clusters of transition-metal elements containing Ln(III) ions are good candidates as single molecule magnets because of the large and anisotropic magnetic moments of rare-earth ions. In this respect complexes simultaneously containing 3*d*-[Cu(II),[4,5] Zn(II),[6] Co(II), Mn(III),[7] Ni(II)[8]] and 4*f*-[Ln(III)] metals received much attention in the past years. However, relatively few polynuclear clusters containing Ln(III) and Fe(III) have so far been reported. In most of these complexes, Schiff-base[9,10] or cyanide anions participate as bridging ligands, the latter imposing a low-spin configuration to Fe(III).[11] Recently, mixed complexes of Fe(III) with lanthanide cations with bridging carboxylate ligands were reported.[12] Heterotetranuclear carboxylate complexes with a $\{Fe_2Ln_2\}$ core have been shown to behave as single molecule magnets.[12] We have recently reported a series of isostructural compounds of the type $[Fe_3Ln(\mu_3\text{-}O)_2(CCl_3COO)_8(H_2O)(THF)_3]$, where Ln represents most of the available Ln(III) cations and Y(III) as a *pseudo*-lanthanide. These have a butterfly type $\{Fe_3Ln(\mu_3-O)_2\}^{8+}$ core, with the Fe(III) cations all being in the $S=5/2$ high-spin state.[13]

The origin of magnetic interactions in these 3*d*-4*f* compounds is more complicated than those complexes of 3*d* metal ions. With the exception of Ln=Gd(III), the crystal-field interaction dominates and ground state of the Ln(III)

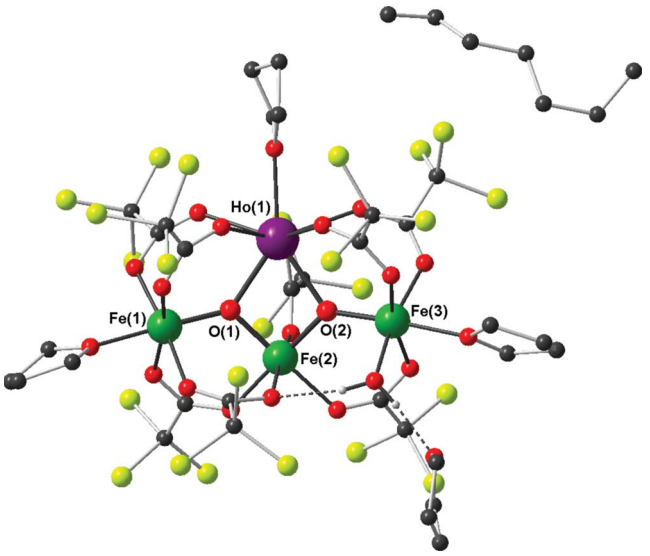

FIG. 1. (Color online) Structure of $[Fe_3HoO_2(CCl_3COO)_8(H_2O)(THF)_3]\cdot THF\cdot C_7H_{16}$ complex.

ions has a first-order angular momentum. To circumvent this problem at low temperature the effective spin approximation for the Ln ground state is applied to interpret the low-temperature magnetization measurements.

The present work describes and discusses the magnetic properties and Mössbauer spectra (MS) of the complexes $[Fe_3Ln(\mu_3\text{-}O)_2(CCl_3COO)_8(H_2O)(THF)_3]\cdot THF\cdot C_7H_{16}$ where Ln represents the heavier lanthanides: Gd(III) (1), Tb(III) (2), Dy(III) (3), Ho(III) (4), Y(III) (5), and Lu(III) (6). The Y atom is not a lanthanide, but is chemically close, and is considered in this paper as such. The synthesis and structure of the compounds are briefly reviewed, and the magnetic properties and Mössbauer spectra are shown, analyzed, and discussed.

II. SYNTHESIS AND STRUCTURE

All six tetranuclear trichloroacetates were obtained[13] by an exchange reaction of the iron-barium μ_3-oxo trinuclear compound $[Fe_2BaO(CCl_3COO)_6(THF)_6]$ (Ref. 14) with the corresponding Ln(III) nitrates in acetone. After removal of barium nitrate and evaporation of acetone, crystals were obtained from a THF:heptane (5:1) mixture. The yield is high (~85%) and the method of synthesis is reproducible. Complexes 1–6 are brown crystalline substances, poorly soluble in water but readily soluble in a variety of polar organic solvents; they can be recrystallized from THF-heptane mixture without change in their composition. The complexes are stable to storage in air under normal conditions.

Compounds 1–6 crystallize isomorphously in the monoclinic space group $P2_1$, with the tetranuclear $[Fe_3Ln(\mu_3\text{-}O)_2(CCl_3COO)_8(H_2O)(THF)_3]$ complex, a THF molecule and an *n*-heptane molecule in the asymmetric unit. The structure of the Fe_3Ho complex 4 is shown in Fig. 1 as an example. The tetranuclear entity has a "butterfly" type structure, with two $Fe_2Ho(\mu_3\text{-}O)$ triangular wings sharing a Ho-Fe body and a dihedral angle between the wings of 146.5°. The metals are thus bridged by two μ_3-oxo centers and eight carboxylate ligands.

TABLE I. Bond lengths (Å) and angles (°) in the $\{Fe_3Ln(\mu_3\text{-}O)_2\}$ cores of 3 and 4 (Ref. 13).

	3 (Ln=Dy)	4 (Ln=Ho)
Ln(1)-O(1)	2.287(4)	2.269(4)
Ln(1)-O(2)	2.300(4)	2.305(5)
Fe(1)-O(1)	1.833(5)	1.840(4)
Fe(2)-O(1)	1.866(4)	1.881(5)
Fe(2)-O(2)	1.887(4)	1.896(4)
Fe(3)-O(2)	1.820(5)	1.825(5)
Ln(1)-O(1)-Fe(1)	132.2(2)	133.1(2)
Ln(1)-O(1)-Fe(2)	100.7(2)	101.07(18)
Fe(1)-O(1)-Fe(2)	125.5(2)	124.4(2)
Ln(1)-O(2)-Fe(3)	130.3(2)	131.1(2)
Ln(1)-O(2)-Fe(2)	99.61(19)	99.3(2)
Fe(3)-O(2)-Fe(2)	130.0(2)	129.5(3)
$LnFe_2/Fe_2Ln$ dihedral angle	146.04(3)	146.51(3)

Selected bond distances and angles for compounds 3 and 4 (Ref. 13) are given in Table I. Each Fe center has a distorted octahedral coordination environment composed of six oxygen donor atoms. However, the precise donor set is different for each iron. Fe(1) has four carboxylate oxygen atoms forming a coplanar equatorial array, with a THF oxygen and an oxo ligand mutually *trans* to each other completing the set. The environment of Fe(3) is closely similar, but one of the four carboxylate oxygens has been replaced by the oxygen of the aqua ligand. Fe(2) has a significantly different environment, with the two (μ_3-O) ligands *cis* to each other, and the remaining four sites occupied by carboxylate oxygens. The bond lengths and angles in one $Fe_2Ln(\mu_3\text{-}O)$ wing are also similar to those in the other wing, so for the magnetic analysis it is justifiable to assume mirror symmetry for the $Fe_3Ln(\mu_3\text{-}O)_2$ core [Fig. 2(a)]. Fe(1) and Fe(3) are located at the wing tips and are denoted as Fe_w, while Fe(2), in the body, is designated Fe_b. The tetranuclear complexes are well separated in the crystal (the distance between molecular units is larger than 15 Å), with no obvious magnetic pathways between them. We can therefore consider the molecules as magnetically independent units.

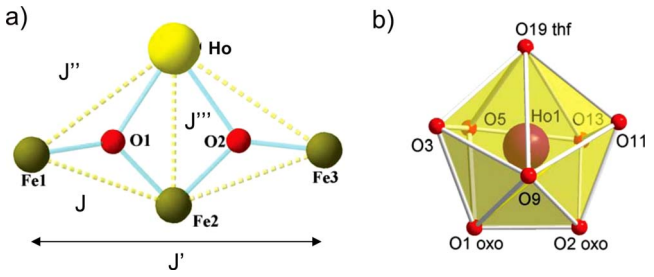

FIG. 2. (Color online) (a) The $\{Fe_3HoO_2\}$ core of (4) compound and the defined interatomic exchange parameters. (b) The symmetry of nearest-neighbor environment of Ho in $[Fe_3HoO_2(CCl_3COO)_8(H_2O)(THF)_3]\cdot THF\cdot C_7H_{16}$ complex.

To model the molecule as a magnetic entity the assumption of mirror symmetry of the "butterfly" on the plane containing the edge is adopted [Fig. 2(a)]. One may also consider the magnetic core as formed by a triangular pyramid where the basis is an obtuse isosceles triangle with the three Fe(III) located at the vertices, and Ln located at the pyramid apex, a convenient description for the analysis below.

III. EXPERIMENTAL

The magnetic ac susceptibility was measured on a MPMS SQUID magnetometer with ac option (Quantum Design). The measurements were done at an excitation frequency in the range of $f=10-1500$ Hz and amplitude of 4 Oe. The magnetization versus field $M(H)$ was performed on a PPMS measurement platform with vibrating sample magnetometer option, at a temperature of 1.8 K and a field up to 90 kOe.

The Mössbauer spectra (MS) were acquired using a constant acceleration spectrometer with symmetrical waveform. A ^{57}Co (1.0 MBq) source has been used. The MS in applied field were obtained in a field oriented perpendicular to the gamma radiation direction and parallel to sample holder. Temperature-dependent Mössbauer measurements (15–295 K) have been done with the sample in a closed cycle cryostat, while those at 3 K without or in applied field (up to 70 kOe) were performed in a He-bath cryostat. The fitting of spectra was performed with NORMOS program, already long time commercially available and the details on procedures are provided for each case in the following chapters. In the presence of a field (B) at nucleus, the quadrupole shift appears as a projection ε related to quadrupole splitting in the paramagnetic region with the following relationship: $\varepsilon = \frac{1}{2}$ QS $(3\cos^2\varphi - 1)$. Depending on the angle, ε it may be positive or negative taking values from $-\frac{1}{2}$ QS (perpendicular to B) up to QS (parallel to B).

IV. MAGNETIC PROPERTIES

A. Ln=nonmagnetic: Y and Lu

The ac and dc magnetic susceptibility measurements at high temperature of the R=Y and Lu compounds fit well to a Curie behavior. The experimental values of χT tend to a monotonous behavior above 4.2 K, which is quite similar for both Y and Lu (4.5 and 4.0 emu K/mol, respectively), as can be observed in Figs. 3(f) and 3(g) data. This value is much lower than the calculated value (13.1 emu K/mol) for three independent Fe(III), taking into account $g=2$ and $S=5/2$, as expected for an Fe(III) ion in its highest spin configuration as was confirmed by Mössbauer spectroscopy.

The $M(H)$ curves (Fig. 4) of the Y and Lu compounds go along together excellently to a saturation value very near to 5 μ_B. From this value one may conjecture that the ground state of the three Fe atoms in the cluster is that of three coupled Fe(III) $S=5/2$ moments, yielding to a total spin of the cluster of $S_{tot}=5/2$ (Fig. 4, triangles and squares). This gives a very robust set of data to consider the Fe_3 cluster as a magnetic self unit.

The $\chi(T)$ and $M(H)$ curves were calculated by means of the MAGPACK code kindly provided by the group of

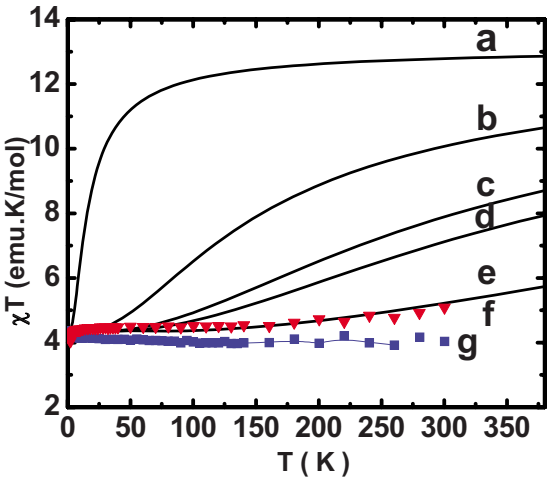

FIG. 3. (Color online) Predictions of the $\chi T(T)$ curves compared to the experimental data. (a) ($J=-1$ K, $J'=0$), (b) ($J=-10$ K, $J'=10$), (c) ($J=-20$ K, $J'=20$), (d) ($J=-25$ K, $J'=0$), (e) ($J=-50$ K, $J'=0$), (f) Experimental data for $\{Fe_3YO_2\}$ cluster (■), and (g) for $\{Fe_3LuO_2\}$ cluster (▼).

Valencia.[15] The hypotheses of this package are that all constituent magnetic centers possess well-isolated orbital nondegenerate ground states. In this case, the leading term of the exchange Hamiltonian is the Heisenberg–Dirac–Van Vleck term. The program calculates the eigenvectors and eigenvalues of the cluster exchange interaction Hamiltonian

$$H_{\text{Fe3-triangle}} = -2J(\vec{S}_1 \cdot \vec{S}_2 + \vec{S}_2 \cdot \vec{S}_3) - 2J'(\vec{S}_1 \cdot \vec{S}_3) \qquad (1)$$

under certain assumptions. In first approximation the spin values are fixed, they are considered isotropic, and located at the cluster atomic sites. Exchange interaction parameters are defined to couple pairs of moments. In agreement with Mössbauer data the Fe moments were considered to be $S=5/2$ and isotropic, $g=2$. From the computed eigenvalues and eigenvectors, the code calculates the equilibrium magni-

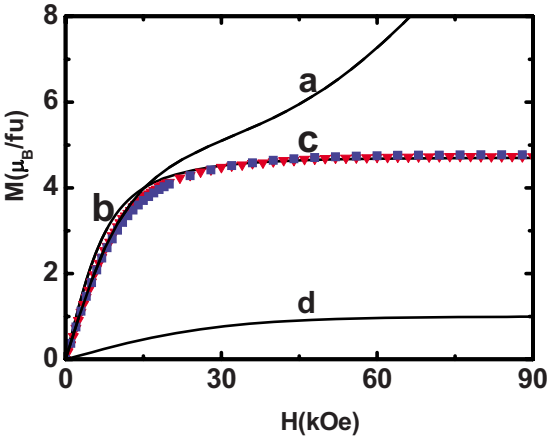

FIG. 4. (Color online) $M(H)$ data of $\{Fe_3YO_2\}$ (■) and $\{Fe_3LuO_2\}$ (▼). The calculated curves for the (+5/2, −5/2, +5/2) cluster spin configuration are shown, for comparison; (a) ($J=-1$ K, $J'=0$), (b) ($J=-20$ K, $J'=0$), (c) ($J=-50$ K, $J'=0$), and (d) ($J=-20$ K, $J'=20$).

tudes of $M(H)$ at fixed temperature and $\chi(T)$ at fixed field. The ground-state multiplet depends on the ratio J/J', ranging from $S_T=0$ to $S_T=5$, as described, for example, in Ref. 16. However, we restrict our analysis to some particular cases of interest in the specific context of the $\{Fe_3LnO_2\}$ clusters. For the sake of clarity we shall describe the spin configuration of the Fe_3 triangle by the triad (sign $S1$, sign $S3$, sign $S2$), where + is up and − is down to the hypothetical easy magnetization direction of the cluster, for total Fe_3 cluster spin $S_T=5/2$. The exchange interaction J between the Fe_w and Fe_b atoms 1–2 and 2–3 is considered identical and antiferromagnetic (AF), while the interaction J' between the Fe_w-Fe_w atoms 1–3 is considered ferromagnetic (F) and negligibly small (Fig. 2). In Fig. 4 some of the calculated curves for $M(H)$ at $T=1.8$ K are shown. If J is small, of the order of 1 K, and $J'=0$, the applied field is capable of polarizing the central spin to the configuration $(+5/2,\ +5/2,\ +5/2)$ for total Fe_3 cluster spin $S_T=15/2$ and $M(H)$ shows an upturn above 20 kOe [Fig. 4(a)]. On the other hand, if J is assumed to be of the order of J' one comes across to a frustrated intermediate spin value. The configuration $(+5/2,\ -5/2,\ +5/2)$ yields an $M(H)$ curve, which is very roughly fitting the experimental data, especially in the rising part, for Ln =Y and Lu, with values in the range $J=-20$ to -50 K, and $J \gg J'$, with $g=1.7$, but no fit is possible for significant values of J' [Fig. 4(d)]. As said above, it is evident that the $M(H)$ data provide information on the ground-state configuration, but is not sensitive enough to determine the actual values of the exchange constants.

With the $(+5/2,\ -5/2,\ +5/2)$ configuration and different values of J' the magnetic susceptibility $\chi(T)$ has been calculated and compared to the experimental results. Here a note of attention is important. The experimental $\chi(T)$ and $M(H)$ have been corrected of diamagnetic contribution according to the equation $\chi^D=-km\times10^{-6}$ emu mol^{-1}, where m is the molecular weight of the compound and k is a factor varying between 0.4 and 0.5.[17] The value $k=0.4$ has been chosen, yielding to $\chi^D=-7.6\times10^{-4}$ emu mol^{-1}, and $\chi^D=-7.9\times10^{-4}$ emu mol^{-1} for the $\{Fe_3YO_2\}$ and $\{Fe_3LuO_2\}$, respectively. The actual value of this correction affects very sensibly the value of J. As best fit to the corrected $\chi T(T)$ the values $J'=0$, $J\approx-50$ K have been obtained [Fig. 3(e)]. On the other hand, the correction to $M(H)$ is within the experimental error bar.

One may conclude from the result of the simulations to the available data that at all measured temperatures the configuration of the Fe_3 triangular magnetic unit maintains the spin configuration $(+5/2,\ -5/2,\ +5/2)$. The Fe(1)-Fe(2) and Fe(2)-Fe(3) pathways have the same μ_3-oxo bridge, but in the former two bridging carboxylate groups connect the two irons, while in the latter there is just one of these bridges. In spite of this difference, the two exchange paths have been approximated to be identical.

A value of $J\approx-50$ K for the Fe(III)-μ-oxo-Fe(III) exchange path is very close to the range of values found for tetranuclear carboxylate compounds with a tetranuclear $\{Fe_4O_2\}$ core. The exchange interactions found with that core[18–24] range from $J=-47.3$ K for $[Fe_4O_2(O_2CPh)_8(phen)_2]$ (Ref. 18) to $J=-65.5$ K for $[Fe_4O_2(O_2CMe)_7(bpy)_2]ClO_4$ (Ref. 23), being, on average, $J=-52$ K. Besides, in a recent work we have found in $[Fe_4O_2(CCl_3COO)_8(THF)_2(DMF)(H_2O)]\cdot THF$, with the same butterfly type of core, an interaction of $J=-45.2$ K.[25] All these results for homotetranuclear complexes are in excellent agreement with the value $J=-50$ K found in this paper for the same interaction path in the heterotetranuclear $\{Fe_3LnO_2\}$. The Fe_b-Fe_b interaction has been found to be on average about $J_{bb}\cong9$ K, therefore much lower than J between Fe_w-Fe_b. In fact, in the $[Fe_4O_2(O_2CMe)_7(bpy)_2]ClO_4$ compound it was shown that the actual value of J_{bb} does not affect the χT temperature dependence.[23] One may conclude that the carboxylate groups have a marked role as pathways in exchange interaction between magnetic ions.

The Fe(III)-O-Fe(III) exchange path in μ-oxo bridges has been studied in polynuclear clusters, in particular in Fe_6 ones, by the use of calculated interaction constants as starting parameters of the thermomagnetic magnitudes.[26] In that study, a semiempirical method to evaluate the J value for a given path, comprising the averaged Fe(III)-O distance over the two bonds (r), and the bond angle (φ), was proposed: $J=A(B+C\cos\varphi+\cos^2\varphi)\exp(Rr)$ [Eq. (8) in Ref. 26].

Taking $A=-2.88\times10^7$ K; $B=0.2$, $C=-1$, and $R=-7$ Å^{-1}, as proposed in that paper, and the distances and angles from Table I, one predicts, $J_{1-2}=-77$ and -69 K, and $J_{2-3}=-69$ and -87 K, for the $\{Fe_3DyO_2\}$ and $\{Fe_3HoO_2\}$, respectively. The average value $J=-50$ K determined from the present measurements is obtained by substituting $R=-7.2$ Å^{-1} in the equation above. At any rate, although one should not overestimate the predicting value of the semiempirical model, it gives reasonable values of J as a function of the geometry of the bond, which plays the main role in the Fe(III)-O-Fe(III) interaction.

B. Ln magnetic: Ln=Gd

From the $M(H)$ data measured at 90 kOe one obtains the value $M_s=11.6$ μ_B (Fig. 5), which coincides excellently with the sum of the saturation value of free Gd, $^8S_{7/2}$, $g=2$, and $M_S=4.7$ μ_B found for the Y or Lu compounds. This means that at 90 kOe the Gd moment is totally polarized in the direction of the maximum applied field. On the other hand, at lower fields the experimental $M(H)$ is lower than the simple sum of the Fe_3 contribution (considered identical to that found for the Y or Lu compound) with the free Gd Brillouin function (curve e in Fig. 5). This result implies that the Gd and the Fe_3 subcluster are coupled by an effective antiferromagnetic exchange constant.

The configuration of the Fe triangle as $(+5/2,\ -5/2,\ +5/2)$, with the exchange parameter $J=-50$ K, identical to the Y and Lu compounds has been assumed to calculate the $M(H)$ curve with MAGPACK, and in addition two different Ln-Fe interactions, $J''=J_{\text{Gd-Fe1–3}}$ for the Gd interaction with Fe_w moments, and $J'''=J_{\text{Gd-Fe2}}$ for its interaction with the Fe_b moment have been introduced (see Fig. 2). The corresponding Hamiltonian term is added to Eq. (1)

$$H_{\text{cluster}}=H_{\text{Fe}_3\text{-triangle}}+H_{\text{Ln-Fe}}=H_{\text{Fe}_3\text{-triangle}}-2J''(\vec{S}_{\text{Ln}}\cdot\vec{S}_1+\vec{S}_{\text{Ln}}\cdot\vec{S}_3)-2J'''(\vec{S}_{\text{Ln}}\cdot\vec{S}_2), \quad (2)$$

where $S_{\text{Ln}}=7/2$ for Ln=Gd. The $M(H)$ predicted curve, at

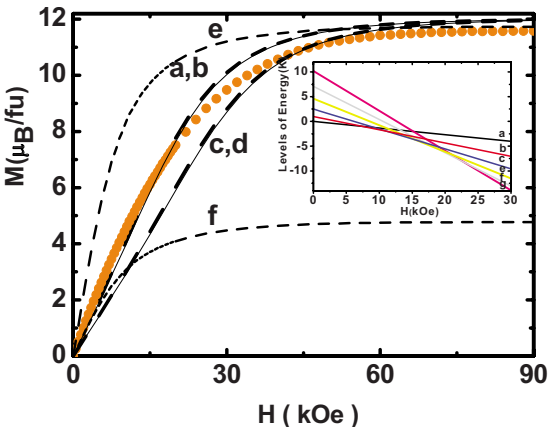

FIG. 5. (Color online) $M(H)$ experimental data for $\{Fe_3GdO_2\}$ (●) compared to the predictions with parameter sets: (a) ($J''=-0.15$ K, $J'''=0$) and (b) ($J''=0$, $J'''=0.35$ K) give rise to curves that fit nicely up to $H=20$ kOe, while for (c) ($J''=-0.15$ K, $J'''=0.15$ K) and (d) ($J''=0$ K, $J'''=0.5$ K) the curves fall lower in the same region, (e) the prediction for the Fe_3 magnetic self unit and the Gd free (uncoupled) ion, and (f) the $\{Fe_3LuO_2\}$ contribution. Inset: ground-state level scheme as a function of the applied field. Note level crossings from the $S=1$ (line a) to the $S=6$ state (line g).

$T=1.8$ K, conforms to the experimental decrease with respect to the Brillouin function for $S=J=7/2$ only for values of $J''\leq 0$ and $J'''\geq 0$. The set of parameters (a) ($J''=-0.15$ K, $J'''=0$) and (b) ($J''=0$, $J'''=0.35$ K) give rise to curves that fit nicely up to $H=20$ kOe [Figs. 5(a) and 5(b)], while for (c) ($J''=-0.15$ K, $J'''=0.15$ K) and (d) ($J''=0$ K, $J'''=0.5$ K) the prediction departs more from the experiment at lower fields (see Fig. 5, curves c and d).

On the other hand, the $\chi(T)\cdot T$ predictions for the set (c) or (d) approaches the experimental data with the same degree of agreement, while for (a) or (b) the curves depart from the experiment at 20 K. Apparently there are quite a number of J'' and J''' pairs that may yield an equally satisfactory fit (see Figs. 5 and 6).

From the systematic study of the evolution of the $M(H)$ curves one comes to the conclusion that the exchange constants J'' and J''' need to be antiferromagnetic and ferromagnetic, respectively. From the MAGPACK calculations one obtains that the low energy multiplet of the electronic states of the tetramer has six functions $|S,M\rangle$ with total spin $S=1$ to 6, with $S=1$ lying lowest in energy and the excited levels differing by approximately 1 K. Therefore, at temperatures where the excited state is much higher than k_BT value, the ground-state spin configuration would consist of the Gd moment parallel to the Fe_b and antiparallel to the Fe_w's, yielding to $S=1$ ground state, with triplet spin degeneracy. As the field is increased, the Zeeman interaction of the external field with the spin-only functions splits the levels by $H_Z=-g\mu_B HM$, and as a consequence the split lowest levels from the excited states get across the other levels to become the ground state (Fig. 5, inset). This course is progressive in steps of $\Delta M=1$, up to $M=6$ for fields above 22 kOe (for the actual set of interaction parameters used), inducing the effect that the $M(H)$ curve below 20 kOe has a nearly linear dependence with the field. At the highest field measured, $H=90$ kOe, the ground state is definitely $|S=6,\ M=6\rangle$, yielding to a saturation value $M_s=12\ \mu_B$; that is, the field polarizes both the net moment of the Fe_3 group and of the Gd in its direction.

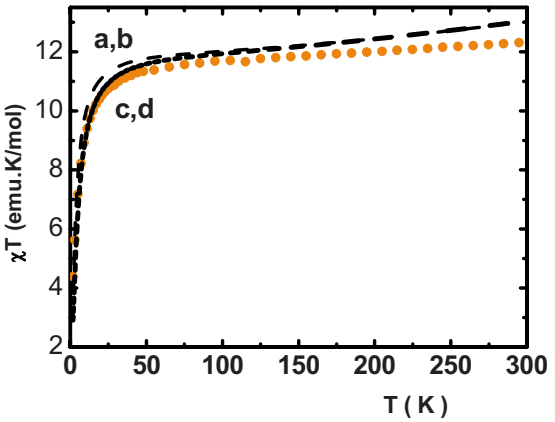

FIG. 6. (Color online) $\chi T(T)$ experimental data for $\{Fe_3GdO_2\}$ (●) compared to the predictions: (a) ($J''=-0.15$ K, $J'''=0$), (b) ($J''=0$, $J'''=0.35$ K), (c) ($J''=-0.15$ K, $J'''=0.15$ K), and (d) ($J''=0$ K, $J'''=0.5$ K).

Since the ground state of the Fe_3 triangle is very robust, i.e., it remains unchanged even at the highest temperatures and applied fields, the quantum-mechanical behavior of its wave functions are equivalent to those of a single $S=5/2$ spin and the triangle spin state may be substituted by just one effective spin $S_{tri}=5/2$. In this case, the computational problem is simplified to that of a Ln-(Fe_3-triangle) pair and the Hamiltonian is reduced to

$$H_{cluster}=-2J_{eff}(\vec{S}_{Ln}\cdot\vec{S}_{tri}). \quad (3)$$

A fit of the $M(H)$ and $\chi(T)$ data can be achieved with just $J_{eff}=-0.35$ K as parameter (Table III).

The values of $J''=J_{Gd-1-3}\approx -0.15$ K and $J'''=J_{Gd-2}\approx 0.35$ K are pretty weak. In the binuclear vantrenFeGd$(NO_3)_3\cdot 2H_2O$, where a high spin Fe(III) ($S=5/2$) couples ferromagnetically with a Gd(III) ion ($S=7/2$) the exchange interaction $J_{Gd\text{-}Fe}\approx 0.72$ K is found,[9] which is larger and ferromagnetic, probably due to the different exchange pathway.

C. Ln magnetic: Ln=Tb, Dy, and Ho

1. High temperature

From the previous section one may conjecture that, in general, the exchange interactions between the Fe atoms are larger by 2 orders of magnitude than the Ln-Fe interactions and the latter reach an exchange energy $E_{Ln\text{-}Fe}$ of a few kelvin. Therefore, at temperatures much higher than $E_{Ln\text{-}Fe}$ the Ln moment and the Fe_3 triangle should behave in the first approximation as decoupled magnetic entities and

$$\chi T=(C_{Fe3}+C_{Ln}), \quad (4)$$

where C_{Fe3} is the Fe triangle unit paramagnetic Curie constant and C_{Ln} is the lanthanide contribution; i.e., $C_{Ln}=g_J^2J(J+1)/8=\mu_{eff}^2/8$, with J being the total angular moment

TABLE II. Experimental values of χT (emu K/mol) determined from ac susceptibility measurements at 150 and 300 K, and from the slope of the $1/\chi$ versus T plots. $\chi_{\text{theo}}T=C_{\text{Fe}_3\text{Lu}}+g_J^2J(J+1)/8$ (error 1%).

Ln	χT (150 K)	χT (300 K)	χT (from slope)	$\chi_{\text{theo}}T$
Y	4.50	5.1		4.0
Gd	11.7	13.1	12.2	11.9
Tb	14.6	15.2	15.6	15.8
Dy	16.1	16.1	16.2	18.2
Ho	18.3	19.2		18.0
Lu	4.0	4.0	4.0	4.0

of the free ion ground state, under the assumption that crystal field (CF) effects are small relative to the thermal energy. This hypothesis may be checked by deducing from experiment the Curie constant and comparing it with the prediction.

The Fe_3-triangle contribution has been experimentally determined from the measurements on the $\{Fe_3LnO_2\}$ clusters with Ln=nonmagnetic (see Sec. IV A), where it was proven that the high-temperature values of χT are quite close for the Y and, respectively, Lu compounds (see Table II). The values of χT, for all available $\{Fe_3LnO_2\}$ compounds, measured at 150 K, where the data points are of excellent quality, and at 300 K, where their error is larger and the values tend to increase slightly, have been included in Table II. In Fig. 7 these points are depicted together with the calculated values according with Eq. (4) (connected by the thick line). The points connected by the dashed line correspond to the same approximation, but taking μ_{eff} from external tables.[27] From direct visual inspection it is clear that the assumptions involved in the simplifying hypothesis support rather well the experimental trend. It may be concluded, as in the previous section for Ln=Gd, that at high temperatures the magnetic Ln moments are decoupled from the Fe triangle, or better described, the Ln-Fe exchange interaction energy is smaller than the thermal energy, then the thermal fluctuations overcome the exchange field, therefore their contribution is given by that of an effectively free paramagnetic Ln.

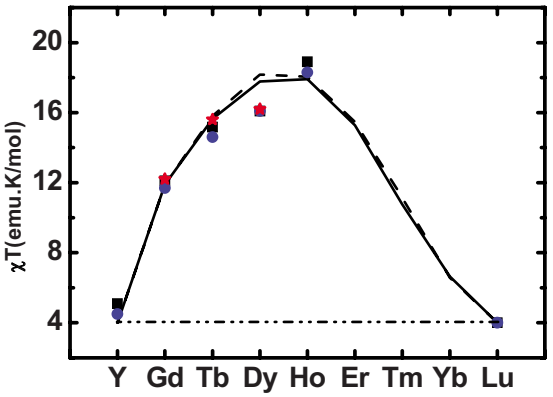

FIG. 7. (Color online) Comparison of the experimental values of the high-temperature experimental values of χT for the different $\{Fe_3LnO_2\}$ clusters, with the calculated values, under the assumption that $\chi T=(\chi\{Fe_3LuO_2\}+\chi_R)T$. (---) reference of $\chi(\{Fe_3LuO_2\}T$; (■) $\chi T(300\ \text{K})$; (●) $\chi T(150\ \text{K})$ (⋆) from $1/\chi v\ T$ slopes; (---) $\chi_R T=g_J^2\ S(S+1)/8$; (—) χT with $\chi_R T=\langle\mu_{\text{eff}}\rangle^2/8$ [table (Ref. 27)].

The $M(H)$ curves at $T=1.8$ K and applied field up to 90 kOe are far from reaching saturation for the Ln=Tb, Dy, and Ho (Fig. 8). Except for Gd, for all compounds with Ln magnetic M_s departs from the free ion limit because of various contributions such as crystal field splitting, spin-orbit coupling, or exchange interactions with the Fe moments (see Fig. 9). Besides, in the case of these three Ln ions the χT curves decrease rapidly with decreasing temperature below 50 K, an indication that there is thermal depopulation of the excited cluster electronic levels (Fig. 10).

2. Low temperature

To interpret the low-temperature data an effective spin Hamiltonian is proposed that describes the quantum characteristics of an anisotropic ground state. For each lanthanide S_{Ln}^* represents the low-temperature effective spin, D is the crystal field parameter for uniaxial symmetry, and $\hat{g}_{\text{Ln}}^*$ is the anisotropic tensor,

TABLE III. Parameters used in the fit of the low temperature $M(H)$ with the effective spin model for the ground state [Eqs. (1)–(3)]. The first block corresponds to the fitting of the $\{Fe_3YO_2\}$ with J for the Fe_w-Fe_b interaction, and $\{Fe_3GdO_2\}$ system with J, J'', and J'''. The fitting of the second block corresponds to fitting $\{Fe_3LnO_2\}$ with J and just an effective exchange constant J_{eff} for the Ln-Fe_3 interaction.

Ln	J (K)	J'' (K)	J''' (K)	J_{eff} (K)	S_{eff}	D (K)	g_x	g_y	g_z
Y and Lu	−50								
Gd	"	−0.15			7/2		2	2	2
	"		0.35		"		"	"	"
	"		0.5				"	"	"
	"	−0.15	0.15				"	"	"
Gd	"			−0.35	7/2		2	2	2
Tb	"			−4	1/2		0	0	25
Dy	"			−5	1/2		14	14	0
Ho	"			−1.6	1	−20	5.1	5.1	8.5

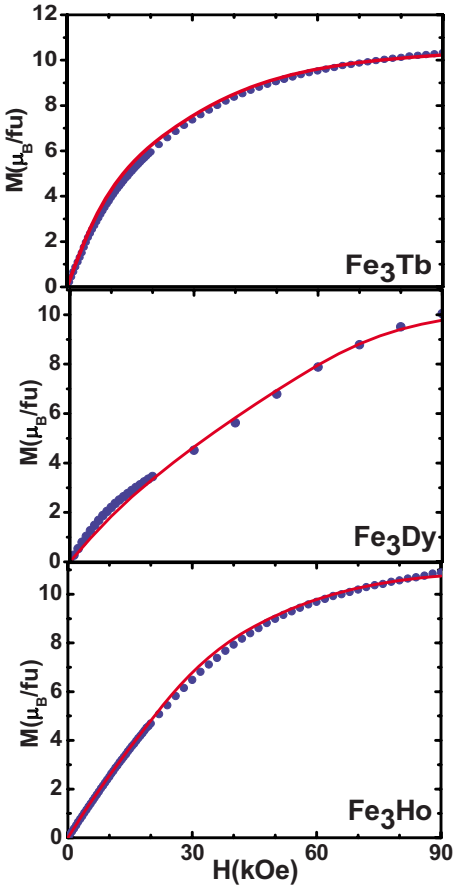

FIG. 8. (Color online) Collected $M(H)$ experimental data (●), at $T=1.8$ K, for heavy Ln series. (—) Calculated predictions with the parameters given in Table III.

$$H_{\text{cluster}} = -2J_{\text{eff}}(\vec{S}^{*}_{\text{Ln}} \cdot \vec{S}_{\text{tri}}) + D\left[S^{*2}_{\text{Ln}} - \frac{1}{3}S^{*}(S^{*}+1)\right] - \mu_{\text{B}}\vec{S}^{*}_{\text{Ln}}\hat{g}^{*}_{\text{Ln}}\vec{H}. \quad (5)$$

In the case of Ln=Tb the free ion ground state is $^{7}F_{6}$. It is a non-Kramers ion with a very anisotropic doublet ground state consisting principally of the $|6,\pm 6\rangle$ states split by a small amount (≈0.2 K in Tb ethylsulphate[28]). In what follows it is approximated to a $S^{*}_{\text{Tb}}=S_{\text{eff}}=1/2$ model. Within this model and based on Eq. (3), the best simulation of the $M(H)$ data presented in Fig. 8 was obtained for $J=-50$ K, and $J_{\text{Tb-Fe3tri}}=J_{\text{eff}}=-4$ K, $g^{*}_{x}=g^{*}_{y}=0$, and $g^{*}_{z}=25$; i.e., axially very anisotropic. Very high values for the effective g_z are not uncommon in Tb.[28] As explained in the previous section, the high-temperature limiting value of $\chi T(T)$ agrees well with the prediction for a paramagnetic free ion Tb decoupled from the Fe_3 cluster.

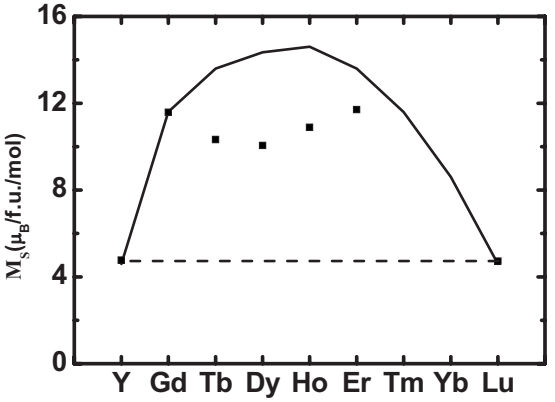

FIG. 9. Comparison of the experimental values (■) of M_s at $H=90$ kOe and $T=1.8$ K, for the different $\{Fe_3LnO_2\}$ clusters, with the M_s calculated by the addition of the free Ln paramagnetic (--) and the Fe_3-triangle saturated contributions (---).

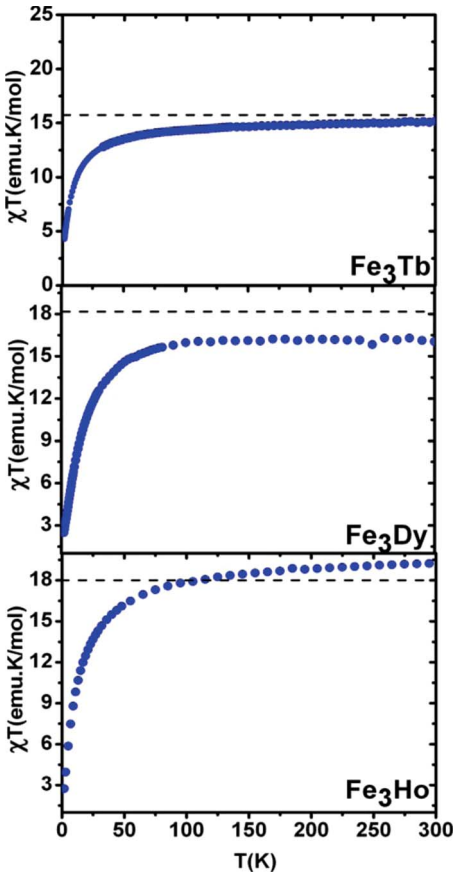

FIG. 10. (Color online) The collected $\chi T(T)$ experimental data (●) for heavy Ln substitutions. (---) The predicted high-temperature limiting value of χT, sum of the paramagnetic free Ln and the Fe_3-triangle contributions is also shown.

The Ln=Dy crystal field splits the $^{6}H_{15/2}$ into Kramers doublets. The first excited level is usually a few tens of kelvin above the ground state, so for the analysis of $M(H)$ at low temperature the magnetic ground state may be considered as an effective $S^{*}_{\text{Dy}}=S_{\text{eff}}=1/2$, with anisotropic g^{*} factors. The best fit (Fig. 8) has been obtained maintaining the interaction parameters within the Fe_3 triangle, $J=-50$ K, and with $J_{\text{Dy-Fe3tri}}=J_{\text{eff}}=-5$ K, $g^{*}_{x}=g^{*}_{y}=14$, and $g^{*}_{z}=0$. This result points to the ground state of Dy as having planar anisotropy. The proposed scheme, therefore, seems to explain quantitatively the experiment, demonstrating again, that the Dy moment is AF coupled to the Fe_3 triangular unit. The actual parameters have to be taken with care, in the absence

of reported data for the magnetically isolated Dy with the same environment. The large values of $g_x^*=g_y^*=14$ have to be understood as acting on the $S_{\text{eff}}=1/2$ doublet, so that if the ground-state doublet is the $|\frac{15}{2},\pm\frac{15}{2}\rangle$ or the $|\frac{15}{2},\pm\frac{13}{2}\rangle$, g has to be scaled correspondingly. The planar anisotropy of the ground state of Dy has been observed in another case, for example, in Dy substituting La in $Ln_2Mg_3(NO_3)_{12}\cdot 24H_2O$.[28]

The Ln=Ho crystal field splitting of the $^5I_8$ ground state is difficult to predict since we have little by-side information. In some cases a value of $S_{\text{Ho}}^*=1$, triplet split into a ground doublet and an excited singlet, has been used satisfactorily.[28] An excellent fit for $M(H)$ is obtained for $D=-20$ K and $J_{\text{Ho-Fetri}}=J_{\text{eff}}=-1.6$ K, and $g_x^*=g_y^*=5.1$ and $g_z^*=8.5$, with $S_{\text{eff}}=1$.

It can be concluded that Ln=Gd, Tb, Dy, and Ho are antiferromagnetically coupled to the Fe_3 triangle, and for Ln=Tb, Dy, and Ho the crystal field interaction plays a relevant role in the description of the ground-state magnetism of the $\{Fe_3LnO_2\}$ clusters. The contributions to M_s are also reduced with respect to the free Ln moment prediction. This can be explained as orbital moment quenching due to the CF effect and giving rise to a ground state of expected reduced moment value (Fig. 9). The experimental $M(H)$ are in all cases lower than the sum of the $M(H)$ of $\{Fe_3LuO_2\}$ and the corresponding Brillouin function for the free Ln moment. This implies that the coupling is antiferromagnetic, as above settled.

As can be observed for $\{Fe_3TbO_2\}$ the χT product tends to approach the value calculated for free paramagnetic Ln and Fe_3 triangle contribution. In the case of Dy compound the attained level remains by 10% lower, while for Ho containing molecule the curve crosses that limit just above 100 K. This behavior supports the differences observed in the $M(H)$ measurements as well as in following presentation including the Mössbauer part.

The low-temperature ac susceptibility shows slow magnetic relaxation phenomena only for Ln=Tb, Dy, and Ho, while no such effect can be observed either for Ln=Y, Lu, or Gd. This phenomenon is clearly related to the magnetic anisotropy specific to Tb, Dy, and Ho lanthanides, since it is absent for the isotropic Ln=Gd tetranuclear compound. This result is shown in Fig. 11 (insets), where χ'' the out-of-phase component of the susceptibility has a strong frequency dependence below 3 K down to the lowest measured temperature 1.8 K. Unluckily, the expected maximum due to blocking could not be observed down to this temperature, however, it is a robust indication of the slow relaxation expected for a single molecule magnet (SMM). Under the assumption that the SMM relaxation has just one characteristic time, corresponding to a Debye relaxation process driven by one activation energy E_a, the relaxation time τ may be written in terms of an Arrhenius law, $\tau(T)=\tau_0\exp(E_a/k_BT)$. The compliance of the Kramers-Kronig equations, $\chi'=\chi_0\frac{1}{1+\omega^2\tau^2}$ and $\chi''=\chi_0\frac{\omega\tau}{1+\omega^2\tau^2}$. Here $\chi_0=\chi_T-\chi_{\text{ad}}$, χ_T is the isothermal equilibrium value, χ_{ad} is the adiabatic susceptibility, and ω is the experimental ac field exciting frequency, which allows to obtain the relation $\chi''/\chi'=\omega\tau$. Substituting $\tau(T)$ and applying natural logarithms one obtains the relation

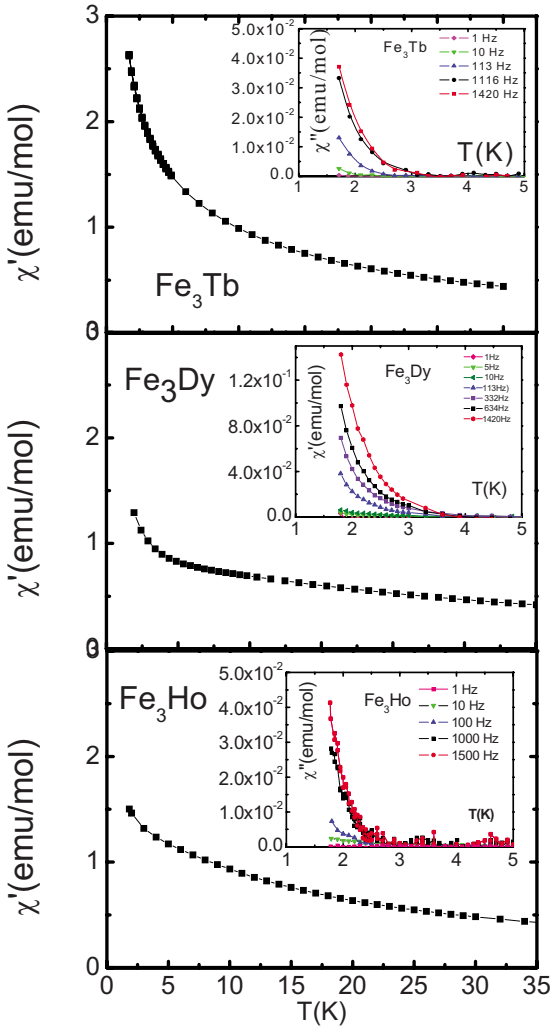

FIG. 11. (Color online) Collected ac susceptibility for heavy Ln substitutions, as a function of frequency, χ', real component. Inset, χ'', out-of-phase component.

$$\ln(\chi''/\chi') = \ln(\omega\tau_0) + E_a/k_BT, \tag{6}$$

which allows to evaluate roughly E_a and τ_0. This methodology has been applied earlier in the determination of τ in Mn_{12} acetate.[29] In Fig. 12 the data for $\{Fe_3DyO_2\}$ are shown as an example. By fitting the experimental χ''/χ' data to Eq. (6), the parameter values $E_a\approx 8\pm 0.5$ K, 9 ± 0.5 K, and 11 ± 0.5 K for the Ln=Tb, Dy, and Ho compounds, respectively, and $\tau_0\approx 10^{-7}$ s were obtained. A more precise result must wait for very low-temperature measurements ($T<1$ K).

V. MÖSSBAUER SPECTRA

All synthesized tetra-nuclear compounds were investigated by Mössbauer spectroscopy at several temperatures. In the following, selections of the most interesting and relevant cases or features are shown.

For the sake of a precise description, the field produced at the nucleus of the central Fe by the own magnetic moment and the magnetic interactions of the blocked spins of neigh-

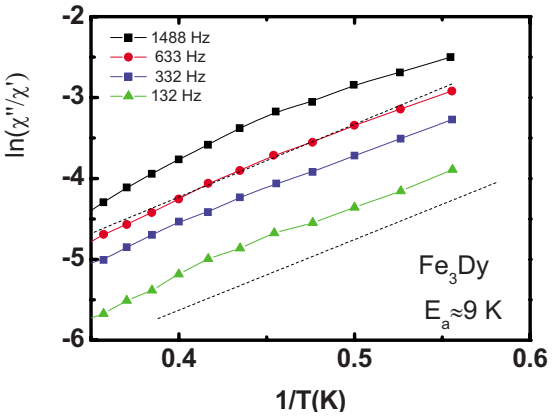

FIG. 12. (Color online) Natural logarithm of the ratio of χ'' over χ' versus $1/T$ of the data for $\{Fe_3DyO_2\}$ given in Fig. 11. (---) Slope corresponding to activation energy E_a=9 K.

boring ions will be named internal field, B_{int}, while the field observed in the presence of external applied fields (B_{appl}) is considered an effective field, B_{eff}, and are related via vector summation:

$$\boldsymbol{B}_{eff} = \boldsymbol{B}_{int} + \boldsymbol{B}_{appl}.$$

Excepting the polarization of the *s* electrons by the own spin, B_{int} includes two contributions: the one originating in the neighboring Fe atoms and a second from the magnetic Ln, if that is the case.

Figure 13 depicts spectra at 3 K of the $\{Fe_3LuO_2\}$; i.e., containing a nonmagnetic rare-earth element measured without and in applied fields. At B_{appl}=0 there are two very broad sextets, showing the onset of spin blocking but still under strong relaxation, as revealed by the broad linewidth values. The strong collapsing shape of the central pattern, assigned to Fe_b (see subsequent paragraphs), indicates a faster process, compared to the Mössbauer Larmor frequency, than for the spectra of the two other Fe_w (later explained), at the 3 K measurement temperature. The isomer shift IS≈0.36–0.44 mm/s, and quadrupole splitting QS ≈0.72–1.22 (see Table IV), and effective fields in the range of 440–500 kOe [Fig. 14(a)] are typical for Fe(III) with surrounding oxygen bonds, in the highest S=5/2 spin state. Such values or even higher are often encountered in spectra of magnetically ordered spins (spinel and hexagonal ferrites, perovskites, or in orthorhombic structures).

Under increasing applied field (Fig. 13) the linewidth becomes narrower showing discrete values in the range observed in magnetically ordered coordination compounds.[30] The three sextets, each showing different relaxing times as derived from the spectra shape and B_{int} values, have been fitted with equal area ratio. This is in agreement with the availability of three sites equally occupied by Fe(III) ions, as deduced from the structural analysis of the single crystals[12,13] and the proposed ground state from the above described magnetic study. The first peculiarity to be mentioned is that two of the sextets are showing decreasing [Fig. 14(a)] B_{eff} values; i.e., the spectra splitting evolves toward smaller velocity values for increasing applied field, while the third (in

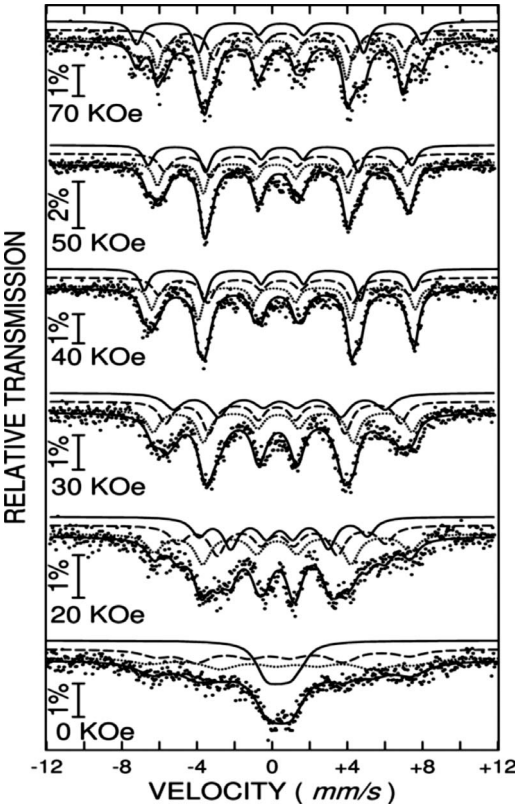

FIG. 13. Mössbauer spectra of $\{Fe_3LuO_2\}$ at 3 K without and with applied fields.

this case the largest split) exhibits an increased value (definitely enlarged distance between external lines of sextet) (Fig. 13). The sextet that depends on the applied field singularly as compared with the other two sextets was related directly to the Fe_b site. Besides, the iron on that site has indirect magnetic interactions via two μ_3-oxo bridge with all other ions, including the two Fe_w, and the spins are less blocked, therefore showing a faster relaxation. Indeed, the opposite trend of B_{eff} in the applied field of the other two sextets compared to that exhibited by the singular behavior of the aforementioned sextet adds evidence to the above statement.

This is a direct and unambiguous microscopic confirmation of the magnetic structure with Fe_b and Fe_w moments to be antiferromagnetically coupled, as established above from $\{Fe_3YO_2\}$ and $\{Fe_3LuO_2\}$ magnetic data. Having in mind that the B_{appl} direction is perpendicular to the gamma radiation direction, and parallel to the sample holder, the increased intensities of the second and fifth lines with increasing external fields indicate the existence of a rotation of the spins in the direction of the applied fields. We will discuss further on this subject later in combination with the MS of the $\{Fe_3TbO_2\}$, $\{Fe_3DyO_2\}$, and $\{Fe_3GdO_2\}$ compounds.

The next figure, Fig. 15, contains spectra versus temperature (at B_{appl}=0) of $\{Fe_3YO_2\}$. It may be expected to observe three Fe patterns (doublets) in the MS, but according to the molecule structure, there are minor differences between the individual surrounding of the two Fe_w sites. Indeed, a good fit of the experimental data was obtained by the contribution of only two doublets with characteristic hyperfine parameters

TABLE IV. Room-temperature Mössbauer fit parameters for some of the $\{Fe_3LnO_2\}$ compounds.

Ln	Pattern	IS (mm/s)	QS (mm/s)	Γ (Mm/s)	Area (%)
Y	Doublet 1	0.44	1.12	0.46	66.67
	Doublet 2	0.33	0.98	0.53	33.33
Gd	Doublet 1	0.46	1.45	0.59	66.67
	Doublet 2	0.36	0.84	0.51	33.33
Dy	Doublet 1	0.43	1.12	0.35	66.67
	Doublet 2	0.31	0.73	0.32	33.33
Tb	Doublet 1	0.45	1.53	0.46	66.67
	Doublet 2	0.39	1.09	0.38	33.33
Lu	Doublet 1	0.44	1.22	0.58	66.67
	Doublet 2	0.36	0.72	0.54	33.33

for Fe(III) in $S=5/2$ state (Table IV). Between 80 and 295 K the two doublets, in a relative area ratio of 2:1, represent the absorption spectra of the very similar two Fe_w sites and, respectively, one Fe_b. Both doublets are showing slightly but noticeable different values of the quadrupole splitting, with IS values in a range characteristic for Fe(III) in its highest spin state, as mentioned above.

Indeed the QS's do not vary between 80 to 295 K; the two fitting doublets provide, at the highest temperature, values of 1.12 mm/s for Fe_w (external doublet) and, respectively, 0.98 mm/s for Fe_b, while the IS are separated by 0.09 mm/s with a higher value of 0.54 mm/s for Fe_w, as can be observed in Table IV, which displays the room-temperature parameters of the Mössbauer doublets of some of the compounds under actual investigation.

It is worth noticing the rather broad shapes of the spectra over the whole range of temperatures. This approach with two doublets implies that in the above compound the electronic states of Fe(III) can be grouped in one pair of almost identical parameters for the two Fe_w sites and a third, distinctive, Fe_b position. In the free fitting procedures (noncorrelated parameters), the large majority of final data yield areas that are close to a 2:1 ratio (66.66% and 33.34%) for doublets and, respectively 1:1:1 ratio for magnetic ordered cases (sextets). Due to rather strong overlapping of patterns, the fittings were performed with correlated area (using the ratios just above mentioned). All the other parameters, the quadrupole splitting (QS), the isomer shift (IS), and linewidth (Γ) (see Table IV for room-temperature values) or the fields at iron nucleus (B_{int} or B_{eff}), for sextet patterns, were noncorrelated in most cases and their behavior as a function of temperature or versus applied field provided very reliable and consistent analysis. It deserves to precise that in the fitting procedures a unique set of specific parameters resulted from the minimized solution of the iteration mathematical process.

The $\{Fe_3GdO_2\}$ compound shows (Fig. 16) pure paramagnetic doublets at 3 K. This is consistent with the lack of Fe spin blocking expected for the low anisotropy barrier of a cluster involving isotropic Gd. At $B_{\text{app}}>20$ kOe the doublets split into three strongly relaxing sextets, which were fitted, accordingly with the above-mentioned approach, with an equal area constraint. For increasing B_{appl}, B_{eff} values for the two Fe_w sextets increase, while that for Fe_b steadily decreases but with a rather low slope [Fig. 14(b)]. This trend is opposite to that observed for $\{Fe_3LuO_2\}$ [Fig. 14(a)] and is singular among the later shown "in field" data of the $\{Fe_3LnO_2\}$ containing heavy rare-earth compounds with Ln =Tb and Dy among the investigated compounds.

The low-temperature (3 K) spectra for $\{Fe_3TbO_2\}$ are revealing spin blocking (Fig. 17) in the absence of applied field (0 Oe) for all Fe sites (three ordered sextets). From the activation energy $E_a=8$ K and $\tau_0=10^{-7}$ s found in Sec. IV C for $\{Fe_3TbO_2\}$ it can be estimated that at 3 K the relaxation time of the system is $\tau\approx 10^{-5}-10^{-6}$ s; i.e., much longer than the Mössbauer spectroscopy characteristic time $\tau\approx 10^{-7}-10^{-8}$ s.[31,32] For this reason the Mössbauer spectra at 3 K and zero field show spins in a blocked state as can be observed by the presence of sextets (Fig. 17). This molecule, as previously demonstrated via magnetic data (Fig. 11), also shows SMM behavior and the presence of magnetic sextets at low temperature in the MS time window confirm the existence of blocked spins. The spectra measured in applied fields were consequently fitted with three sextets (for this compound all Fe sites exhibited blocked spins already "in zero applied field") with equal area ratio. The in field evolution puts in evidence two B_{eff} decreasing, for the Fe_w sites, and the third, B_{eff} for Fe_b, increasing and overpassing the former two [Fig. 14(c)]. The reason for this blocking lies in the large anisotropy of Tb, which is coupled to the Fe_3 triangle, which was evidenced in the fitting of the $M(H)$ curves at 1.8 K, giving an effective hindering barrier to total spin reversal; i.e., it has incipient SMM behavior, in agreement with ac susceptibility measurements.

The peculiar influence on the Fe_3 subcluster generated by the magnetic Dy in $\{Fe_3DyO_2\}$ is revealed by the spectra (Fig. 18) measured at 3 K at $B_{\text{appl}}=0$ and also acquired with increasing applied field. As for the $\{Fe_3TbO_2\}$ compound, it unambiguously shows spin blocking at $B_{\text{appl}}=0$, again related to the magnetic anisotropy induced by the Dy rare earth. Just as argued for the $\{Fe_3TbO_2\}$ compound, taking the activation energy deduced for $\{Fe_3DyO_2\}$ from the ac susceptibility analysis ($E_a=9$ K), the relaxation time at 3 K is $\tau\approx 10^{-5}-10^{-6}$ s, likewise, much longer than the characteristic Mössbauer time window. Therefore, the spin blocking in this

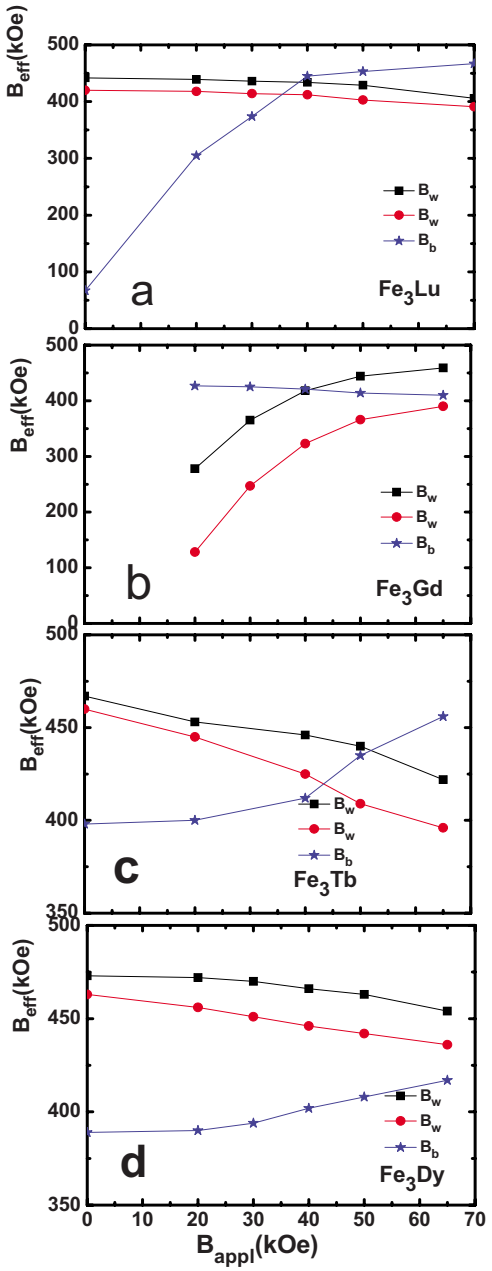

FIG. 14. (Color online) Effective fields (B_{eff}) dependence on applied fields (B_{appl}) for (a) $\{Fe_3LuO_2\}$, (b) $\{Fe_3GdO_2\}$, (c) $\{Fe_3TbO_2\}$, (d) $\{Fe_3DyO_2\}$ with Fe_w (●, ■) and Fe_b (⋆).

case is similar to that in the Tb containing molecule and is related to SMM behavior (Fig. 11).

In an external field of 65 kOe, the B_{eff} value for Fe_b remains below that for the Fe_w, their changes being around 20 kOe only, and this smaller effect is confirmed also by evidently rather minor changes in the intensities of the second and fifth absorption lines in MS, showing a clear resistance of Fe magnetic moments to align themselves along the applied field direction, as observed in the experimental spectra (Fig. 18).

As a resume, we may say that B_{eff} values (400–470 kOe) for the $\{Fe_3TbO_2\}$ and $\{Fe_3DyO_2\}$ samples are in close agreement with hyperfine fields observed for an Fe(III) in octahe-

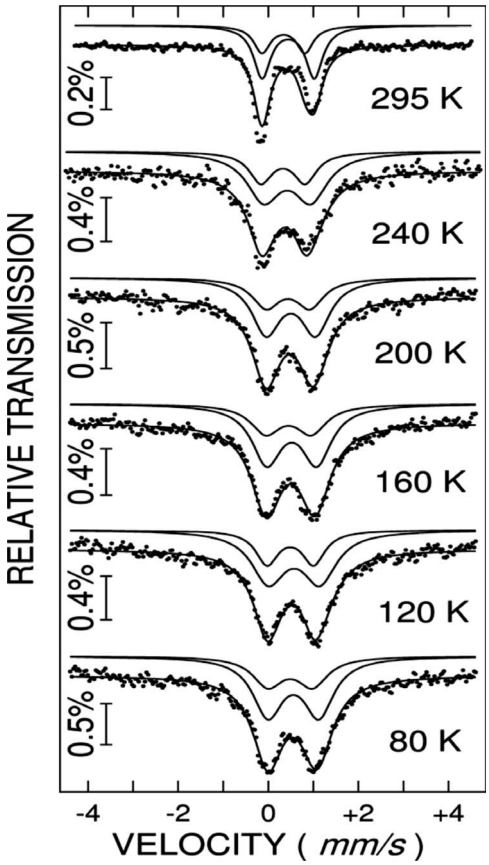

FIG. 15. Experimental Mössbauer spectra at different temperatures and their fits for $\{Fe_3YO_2\}$.

dral oxygen surrounding, in its highest $S=5/2$ spin state.[30] But, nevertheless, these values are smaller by 60–100 kOe than those for highly ionic Fe oxides, a natural effect of the weaker strengths of a coordination bond as compared to an ionic one. In $\{Fe_3LuO_2\}$, $\{Fe_3TbO_2\}$, and $\{Fe_3DyO_2$ the B_{eff}'s in each compound have the same field dependence for the Fe_w and Fe_b sites, the former are decreasing and, respectively, the latter are increasing with increasing field.

The variation in B_{eff} vs B_{appl} intrinsically contains information about both the orientation of the spin with respect to the applied field as well as about spin relaxation mechanisms. In the static case conditions (at low enough temperature so that no relaxation exists), the effect of the applied field is to reorient the cluster spin with respect to its direction. Depending on the coupling inside the cluster, some spins will orient along the field, the others, opposite to the field. Any further increment of B_{appl} will provide either an increasing or a decreasing trend of B_{eff}, due to the addition/subtraction of B_{appl} to/from B_{int}, depending on their relative orientation. Therefore, the dependence of B_{eff} vs B_{appl} is considered in terms of a vectorial model, since more knowledge about the magnetic coupling inside the cluster is retrieved. In the dynamical case (activated magnetic relaxation in the absence of the applied field), the first effect of the field is to freeze the cluster spin by field-induced anisotropy and then to reorient it. Initially the effective field increases under the applied field mainly due to the increment of the time averaged internal field and subsequently by spin reorientation

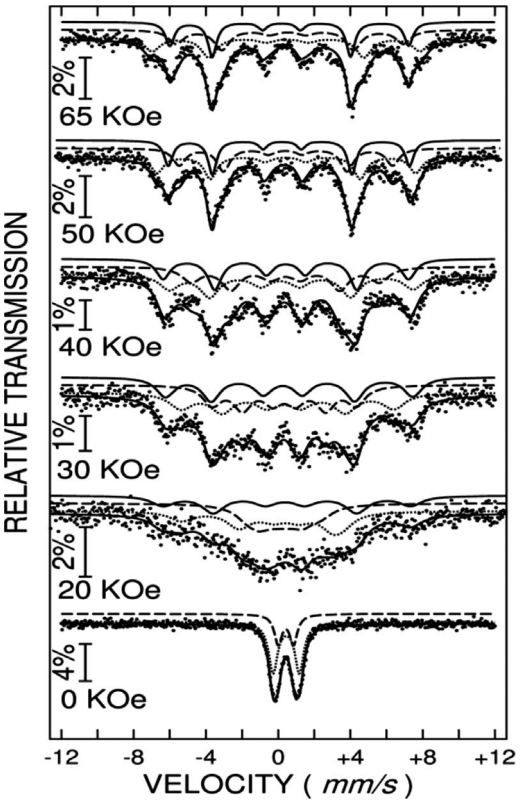

FIG. 16. Representative spectra of $\{Fe_3GdO_2\}$ at 3 K under various applied fields.

and addition/subtraction of the applied field. In the dynamical case a deduction of the B_{int} from B_{eff} and B_{appl} is unachievable. The only unitary treatment for all considered Fe positions concerns the variation in B_{eff} versus B_{appl} (Fig. 14), which in fact is carefully analyzed with the definite purpose to derive data related to spin couplings and magnetic relaxation mechanisms.

In $B_{appl}=0$ the cluster total spin may be derived since the hyperfine field experimented by a high spin Fe(III) (B^0_{int}) is mainly determined by the Fermi contact term, which corresponds to the polarization of the *s* electrons at the nucleus by the electrons in the partially filled *d* shell (half-filled shell configuration due to electron occupation of all five *d* orbitals). In an exchange coupled cluster the internal hyperfine field B_{int} at an Fe site (*i*) with average spin $\langle S_i\rangle$ is $B^{(i)}_{int}=(\langle S_i\rangle/S_{Fe})B^0_{int}$. The cluster total spin in our Fe_3 subcluster, under the conjecture, derived from the magnetic measurements, of strong antiferromagnetic coupling between Fe_w's and Fe_b, would be

$$S=\sum_{i=1-3}\langle S_i\rangle=\frac{S_{Fe}}{B^0_{int}}[B^{(1)}_w-B^{(2)}_b+B^{(3)}_w], \tag{7}$$

with $B^0_{int}=550$ kOe,[32] and $S_{Fe}=2.5$.[33] In the two cases where B_{int} could be determined at $B_{appl}=0$, since the Fe spins are blocked at 3 K, namely for $\{Fe_3TbO_2\}$ and $\{Fe_3DyO_2\}$, and a value $S=2.4\pm0.2$ is obtained, which confirms nicely that the total Fe_3 cluster spin is $S=5/2$ using a high resolution microscopic technique as Mössbauer spectroscopy for ^{57}Fe.

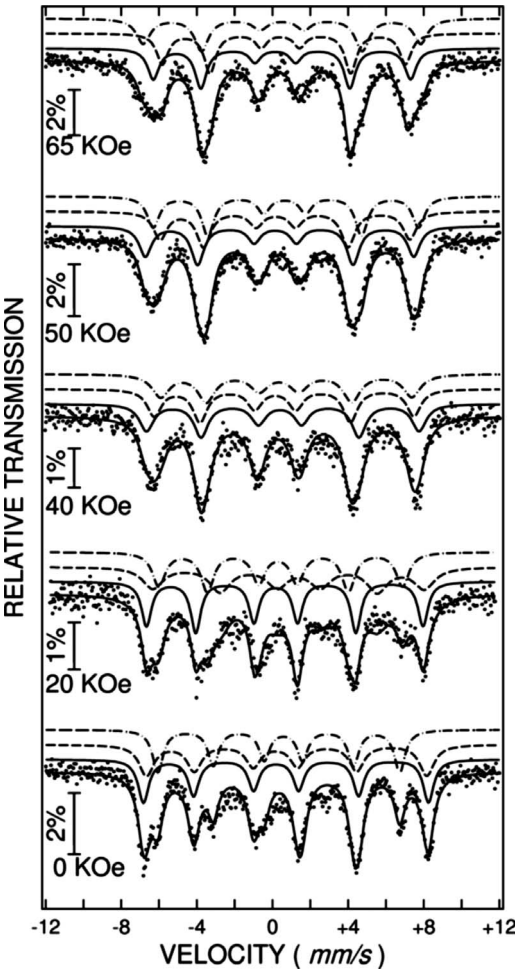

FIG. 17. The Mössbauer spectra of $\{Fe_3TbO_2\}$ at 3 K without and with applied fields.

In $\{Fe_3TbO_2\}$ and $\{Fe_3DyO_2\}$ the applied field orients the total cluster moment, and therefore the two Fe_w moments are polarized in the field direction, while the Fe_b is antiparallel to the Fe_w because of the strong AF intracluster coupling. Since B_{int}, deduced from spin-only contribution (Fermi contact term), is opposite to the magnetic moment at site *i*, μ_i, when a field B_{appl} is applied with a positive projection to μ_i, the effective field B_{eff} decreases with respect to B^i_{int}, and vice versa, when μ_i is opposite to B_{appl}, B_{eff} increases. Therefore, in Ln=Tb and Dy compounds the B_{eff}'s of the two Fe_w's decrease with the field, while that of the Fe_b increases.

Let us denote the increment/decrement of B_{eff} within an applied field from 0 to $|B_{appl}|$ by parameter Δ. Three situations can be distinguished: (i) $\Delta>|B_{appl}|$, when the spin blocking mechanism is caused by the applied field, (ii) $\Delta=|B_{appl}|$, which occurs in the particular case of an applied field along the initial direction of the blocked spins, and (iii) $\Delta<|B_{appl}|$, in the case that spin reorientation effects take place under the applied field. In the whole range of our in field experiments on $\{Fe_3TbO_2\}$ and $\{Fe_3DyO_2\}$, the increment/decrement Δ is smaller than $|B_{appl}|$ since we deal with a randomly oriented powder. However, the fact that in Ln=Tb and Dy compounds the B_{eff}'s of the two Fe_w's decrease with the field while that of the Fe_b increases proves

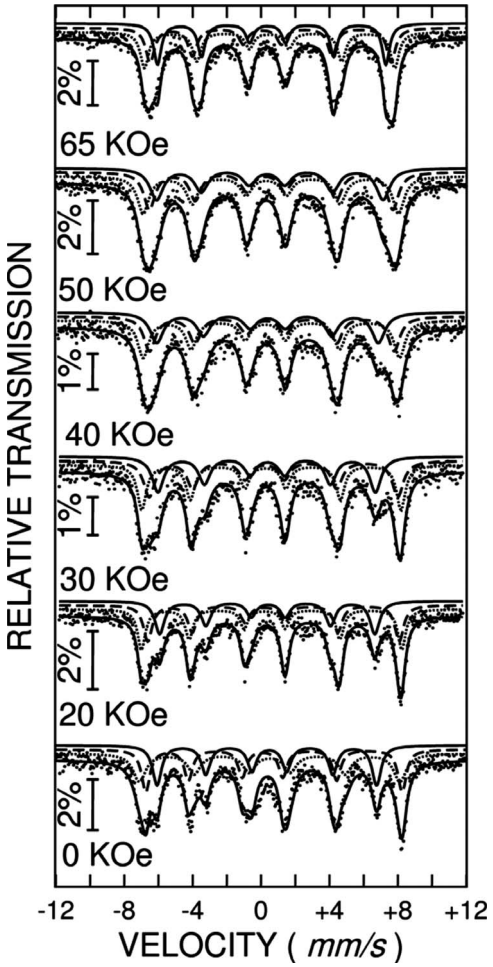

FIG. 18. The $\{Fe_3DyO_2\}$ spectra without or with applied fields at 3 K.

unambiguously that the Fe_3 magnetic self unit consists of two Fe_w's antiferromagnetically coupled to the central Fe_b, giving rise to a cluster total spin $S_T=5/2$. In addition, the fact that Δ is smaller than $|B_{appl}|$ proves that all the three Fe spins of the unit are already blocked at 3 K even in the absence of an applied field. That is in contrast with the $\{Fe_3LuO_2\}$ compound for Fe_b position, where Δ is much higher than $|B_{appl}|$ for applied fields lower than 50 kOe, evidencing a relaxation of spins on that position for small applied fields.

One should keep in mind that hyperfine field at nucleus, B_{int}, is the result of all magnetic contributions of surrounding ions, in this case of three Fe and a magnetic Ln ion, therefore the values of B_{int} on all three positions are different in $\{Fe_3TbO_2\}$ and $\{Fe_3DyO_2\}$ and are related with the coupling of the Ln ion magnetic moment with the Fe_3 unit. At the maximum applied field of 70 kOe (Fig. 14), for $\{Fe_3LuO_2\}$ the Fe_b site shows the largest B_{eff} with respect to those for the Fe_w sites, with its direction parallel to the applied field. For $\{Fe_3TbO_2\}$ B_{eff} value is also larger for the Fe_b site for maximum applied field, but B_{int} is sensibly lower than that for each of the Fe_w sites (see values for $B_{appl}=0$). In contrast, in the $\{Fe_3DyO_2\}$ case Fe_b exhibits the lowest B_{eff}, at the highest applied field, but starting from the lowest B_{int}, thus conserving the mentioned parallel direction. It can be concluded that in the $\{Fe_3TbO_2\}$ case, the effect of applied field on magnetic moments is substantially larger than in the case of $\{Fe_3DyO_2\}$. It may be expected for a highly axial anisotropic ground state yielding to a high moment in the field direction, most probably due to its planar anisotropy, as deduced from the magnetic measurements.

The $\{Fe_3GdO_2\}$ case has a peculiar behavior with respect to the other $\{Fe_3LnO_2\}$, since the B_{eff}'s of the two Fe_w's increase, and that of Fe_b decreases with increasing field. This apparent paradox is elegantly explained with the help of the results in Sec. IV B, where, from the $M(H)$ curve at $T=1.8$ K it was shown that at low fields and low temperature the cluster spin is $S=1$, that is, the $S_{Gd}=7/2$ is antiparallel to the Fe_3 cluster unit spin with $S_T=5/2$. In those conditions the Gd moment establishes the cluster moment orientation: the Gd spin orients along the applied field, the two Fe_w's moments, which are coupled antiparallel to the Gd moment, orient opposite to the applied field, the Fe_b moment orients antiparallel to the Fe_w's moments and hence, parallel to the applied field and Gd moment too. That is exactly an inverse orientation of the Fe_3 cluster unit spin as compared with the other three compounds mentioned above. Therefore, when the field increases, the B_{eff} of the Fe_w's increases and Fe_b, respectively, decreases for the $\{Fe_3GdO_2\}$, opposite to all the other three compounds presented in Fig. 14. However, this behavior of the effective hyperfine fields on the three Fe positions was observed up to fields of 65 kOe, proving that the change in the cluster spin value to $S=6$, as suggested from magnetic data fittings, should be expected above 60 kOe applied field (if it would appear at a lower field, an opposite behavior of the effective field vs the applied field on the Fe_w and Fe_b positions, respectively, would be observed). It is worth mentioning that the value of 22 kOe found for the $S=5-6$ level crossing does not imply that the $S=6$ level is the only one populated. It needs a higher field to mainly populate that level, as is experimentally observed since saturation occurs for fields higher than 60 kOe (Fig. 5), in good agreement with the Mössbauer data of B_{eff} for Fe_w [Fig. 14(b)].

Furthermore, spectra on $\{Fe_3DyO_2\}$ were acquired without applied field (i.e., at $B_{app}=0$) in a temperature range of 80–295 K (Fig. 19). In this temperature range the spectra exhibited an overlapping of two doublets, which were with the already discussed 2:1 area ratio, assigned for the population of Fe_w and, respectively, Fe_b, as expected for a spin unblocked state. The QS values decrease 15% for Fe_w and, respectively, 34% for Fe_b (inner doublet) over a temperature interval of 215 K (80–295 K). Besides, IS shows a linear decrease typical of second-order Doppler shift,[34] but changing its slope at 200 K.

It seems that the observed effect is related to a modification above certain temperature of the sharing time of electrons between Ln, Fe_b, Fe_w, and the four different types of oxygen forming the octahedral coordination around each Fe. In our approach to this problem the crystal field approximation was used taking into account that the charge on the O^{oxo} is δ_1, on the O^{carb} is δ_2, and on the $O^{THF}\approx O^{H_2O}$ is δ_3. The sixfold coordination of the Fe(III) atoms can be schematized as shown in Fig. 20, into two *trans*- and a *cis*- environments,

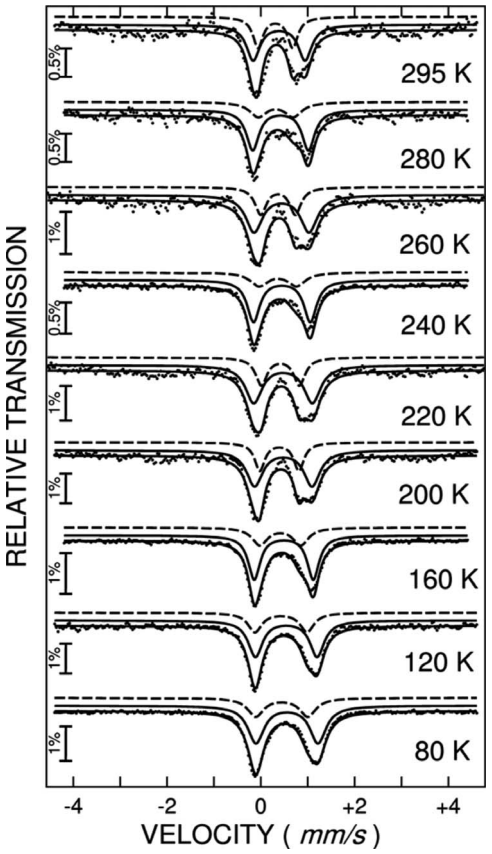

FIG. 19. Selection of Mössbauer spectra at 80–295 K and their fits for $\{Fe_3DyO_2\}$.

the first one assigned to each of Fe_w and the second one to Fe_b, the differences in symmetry being the reason for the observed distinct values of QS. Therefore, one should note that the Fe_b has two sharing μ_3-oxo oxygen in the next neighborhood compared with just one for Fe_w (Fig. 20).

In the Mössbauer spectroscopy literature on homotetranuclear Fe(III) complexes containing carboxylate anions[18–20,23,35–40] are some general characteristic aspects: (i) the geometry of $\{Fe_4O_2\}$ core is presented as bath (_/), nearly plate (---), and armchair (\-\) forms; (ii) the nature of the donor atoms from the environment of Fe are O_6 or $O_{(6-x)}N_x$; (iii) the nature of the molecules coordinated to Fe donor atoms may be different: $O=O^{2-}$ (μ-oxo), $O(H_2O)$, O(OH), O(RCOO); N= (N^{3-}, different Schiff bases, etc.); (iv) the Mössbauer spectra have been fitted with one, two, or

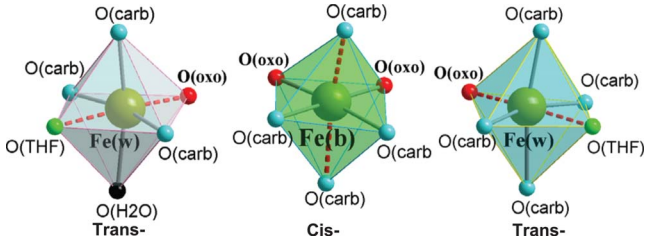

FIG. 20. (Color online) Schematic representation of the nearest environment of the three Fe atoms in $[Fe_3LnO_2(CCl_3COO)_8(H_2O)(THF)_3]\cdot THF\cdot C_7H_{16}$ complexes.

four doublets. As a result, the published Mössbauer spectra parameter data are not strictly comparable. The MS parameters vary within the following limits:

(i) for one doublet:

$$(80\ \text{K}),\ \text{IS} = 0.46 \div 0.52,\ \text{QS} = 0.62 \div 1.21\ \text{mm/s},$$

(ii) for two doublets:

$$\text{doublet 1(body atom):(80 K)},\ \text{IS} = 0.46 \div 0.54,$$
$$\text{QS} = 0.47 \div 0.96\ \text{mm/s}.$$

$$\text{doublet 2(wing atom):(80 K)},\quad \text{IS} = 0.44 \div 0.52,$$
$$\text{QS} = 1.04 \div 1.40\ \text{mm/s},$$

(iii) for four doublets (just one case[19]):

$$(293 \div 80\ \text{K})\ \text{IS} = 0.5 \div 0.54,\quad \text{QS} = 0.44 \div 0.68\ \text{mm/s}.$$

$$\text{QS} = 1.07 \div 1.28\ \text{mm/s}.$$

The data presented above are characteristic for Fe(III) in high spin state ($S=5/2$); i.e., the donor atoms form a weak ligand field. It is noteworthy to later compare with actual results the relative low value of isomer shift (IS $=0.24$ mm/s at 80 K) for doublet 2 of MS found for the complex $[Fe_4(\mu\text{-}O_2)(\mu\text{-BMDP})_2(\mu\text{-OAc})_2](NO_3)_3(OH)\cdot 6H_2O$ where BMDP=N,N,N′-Tris((Methyl)-2-benzimidazolylmethyl)-N′-methyl-1,3-diamino-2-propanol, which indicates a high total *s*-electronic density around the Fe nucleus. This fact allowed Satcher *et al.*[38] to assign this doublet to Fe(III) with coordination number CN=5.

According to the literature data there are just a few heterotetranuclear iron containing μ_3-oxo carboxylates with butterfly core.[12] It is easily observable that our data for doublets appearing in $\{Fe_3YO_2\}$ (Fig. 15, Table IV) and Fe_3Dy (Fig. 19, Table IV) are rather close to values quoted in the literature. The values of the QS are quite in the range or larger than those described above and lower for IS of the inner doublet. In Table IV, the two IS values are specific and distinctly different for each (body or wing) Fe location.

As detailed above, the main difference between the Fe_b and Fe_w surroundings is derived from a *cis*-configuration of the former, with four equivalent oxygen neighbors in the plane and, respectively, *trans*-configuration for the latter, obviously implying nonequivalent bonds both in the plane and on vertical axes of the octahedron. Both the QS and IS are influenced by the specific electron transferability of each of the four types of oxygen ions O^{oxo}, O^{carb}, O^{THF}, and O^{H_2O}, the interionic distances and their coupling bonds playing the crucial role. In this way one may understand the evidently smaller IS for Fe_b and its QS peculiar temperature behavior in all spectra shown. Nevertheless, the lower B^i_{int} observed for Tb and Dy containing tetra-nuclear compounds is also related to a weaker bond with the above-mentioned four types of oxygen as compared with the one existing in purely oxides, thus giving rise to B_{int} of order 500–550 kOe.

In homo-tetra-nuclear iron carboxylates such changes were not observed. This fact permits us to conclude that just the presence of Ln ion in the composition of the molecule

leads to the observed behavior. In this case the contributions of lanthanide atomic orbitals (AO) in the molecular orbitals of the cluster are higher at low temperature than at high temperature. As a result, part of the electron density, which is transferred to the Fe atoms, decreases and it affects more pronouncedly the *s*-atomic orbitals of Fe_b and, respectively, the *d*-atomic orbitals of Fe_w. It is necessary to note that according to the conclusions of Ref. 20, the oxo-oxygen atoms participate only in σ-chemical bonds while the O^{carb} acts with both σ and π ones. Such transfer modifies also the ionic bond strength of the Fe ligand, as it was demonstrated on the oxo-trinuclear iron(III) carboxylates.[41] Another previous work[42] reported that QS increases with Fe(III)–carboxylate bond strength. To clarify various assumptions and how the electron density is distributed on *d*-AO of the Fe, supplementary investigations and calculations are needed.

VI. CONCLUSIONS

Six μ_3-oxo tetranuclear complexes $[Fe_3LnO_2(CCl_3COO)_8(H_2O)(THF)_3]\cdot THF\cdot C_7H_{16}$ with Ln =Gd(III) (1), Tb(III) (2), Dy(III) (3), Ho(III) (4), Y(III) (5), and Lu(III) (6) have been prepared. The magnetic and Mössbauer data were considered in terms of the tetranuclear butterfly type Fe_3-Ln core of the compounds. The antiferromagnetic exchange interaction between two types of Fe location, Fe_w to Fe_b, ($J=-50$ K) was found to be consistent with the Fe-Fe interactions observed in homo-tetranuclear Fe complexes. The Ln-Fe interactions are much weaker. The low-temperature $M(H)$ curves could be explained assuming that the Ln ground state may be represented by an effective spin, which has the quantum-mechanical degeneracy and anisotropy of the crystal field split ground state. The low-temperature ac susceptibility measurements show for $\{Fe_3TbO_2\}$, $\{Fe_3DyO_2\}$, and $\{Fe_3HoO_2\}$ the existence of a slow relaxing process, characteristic for SMM behavior of the cluster moment, with an activation energy $E_a=8$, 9, and 10 K, respectively, corresponding to the compounds with higher anisotropy.

The high spin $S=5/2$ of Fe(III) atoms was ratified, via the IS and B_{int}, provided by Mössbauer investigation, which also detailed the specific interaction on the two different Fe_w and Fe_b locations in the molecule. The Mössbauer in field data proved unambiguously the antiparallel spin orientation of the Fe_b and Fe_w. Besides, at 3 K spin blocking was found to occur in $\{Fe_3TbO_2\}$ and $\{Fe_3DyO_2\}$ in the Mössbauer time window, in agreement with the SMM behavior demonstrated by the ac susceptibility measurements.

Comparing the in field behavior for the four investigated compounds, the B_{eff}'s in $\{Fe_3LuO_2\}$, $\{Fe_3TbO_2\}$, and $\{Fe_3DyO_2\}$, increase for Fe_b and decrease for Fe_w, while in $\{Fe_3GdO_2\}$, the trend is the opposite. This is correlated with the isotropic character of the Gd ion, which is polarized in the direction of the applied field for $B_{appl}\approx 60$ kOe. The lack of anisotropy in this case is also confirmed by the absence of any observable spin blocking at lowest measuring temperature. The temperature dependence, observed both for QS and IS parameters at high temperatures, reflects the influence of four types of oxygen ions O^{oxo}, O^{carb}, O^{THF}, and O^{H_2O} assembling the octahedral Fe surroundings.

ACKNOWLEDGMENTS

We thank I. Ogurtsov for productive discussion of the results and the Valencia group for the MAGPACK code and advice. The authors acknowledge the financial support of the DFG (Center for Functional Nanostructures). This work was also supported by the MAGMANet European Network of Excellence via WP.O9 Package. Substantial financial support of Project No. MAT08/1077 MINCINN (Spain), Project CORINT Grant No. 114/2006, and Project IDEI Grant No. 235/2007 (Romania) is deeply acknowledged.

[1] D. Gatteschi, R. Sessoli, and A. Cornia, Chem. Commun. (Cambridge) **2000**, 725 ; D. N. Hendrickson and R. Sessoli, MRS Bull. **25**, 66 (2000).
[2] D. Gatteschi and R. Sessoli, Angew. Chem. Int. Ed. **42**, 268 (2003).
[3] W. Wernsdorfer, N. Aliaga-Alcalde, D. N. Hendrickson, and G. Christou, Nature (London) **416**, 406 (2002).
[4] A. Bencini, C. Benelli, A. Caneschi, R. L. Carlin, A. Dei, and D. Gatteschi, J. Am. Chem. Soc. **107**, 8128 (1985).
[5] M. Kahn, C. Mathonier, and O. Kahn, Inorg. Chem. **38**, 3692 (1999).
[6] Y. Cui, J.-T. Chen, and J.-S. Huang, Polyhedron **20**, 1795 (2001).
[7] C. Benelli, M. Murrie, S. Parsons, and R. E. P. Winpenny, J. Chem. Soc. Dalton Trans. **1999**, 4126; C. Zaleski, E. Depperman, J. Kampf, M. Kirk, and V. Pecoraro, Angew. Chem. Int. Ed. **43**, 3912 (2004); A. Mishra, W. Wernsdorfer, K. Abboud, and G. Christou, J. Am. Chem. Soc. **126**, 15648 (2004); A. Mishra, W. Wernsdorfer, S. Parson, G. Christou, and E. Brechin, Chem. Commun. (Cambridge) **2005**, 2086.
[8] E. Brechin, S. Harris, S. Parson, and R. E. P. Winpenny, J. Chem. Soc. Dalton Trans. **1997**, 1665.
[9] J.-P. Costes, A. Dupuis, and J.-P. Laurent, Eur. J. Inorg. Chem. **1998**, 1543.
[10] J.-P. Costes, F. Dahan, F. Dumestre, J. M. Clemente-Juan, A. Mari, and J.-P. Tuchagues, Dalton Trans. **2003**, 464.
[11] A. Figuerola, C. Diaz, J. Ribas, V. Tangoulis, J. Granell, F. Lloret, J. Mahia, and M. Maestro, Inorg. Chem. **42**, 641 (2003).
[12] C. I. Turta, D. Prodius, V. M. Mereacre, S. G. Shova, M. Gdaniec, Yu. B. Simonov, V. Kuncser, G. Filoti, A. Caneschi, and L. Sorace, Inorg. Chem. Commun. **7**, 576 (2004); M. Murugesu, A. Mishra, W. Wernsdorfer, K. A. Abboud, and G. Christou, Polyhedron **25**, 613 (2006).
[13] V. Mereacre, D. Prodius, C. Turta, S. Shova, G. Filoti, J. Bartolomé, R. Clérac, C. E. Anson, and A. K. Powell, Polyhedron (to be published).
[14] D. Prodius, C. I. Turta, V. M. Mereacre, S. G. Shova, M. Gdaniec, Yu. A. Simonov, V. Kuncser, G. Filoti, and A. Caneschi, Polyhedron **25**, 2175 (2006).
[15] J. J. Borrás-Almenar, J. M. Clemente-Juan, E. Coronado, and B.

S. Tsukerblat, Inorg. Chem. **38**, 6081 (1999).
[16] D. N. Hendrickson, *Research Frontiers in Magnetochemistry*, edited by C. J. O'Connor (World Scientific, Singapore, 1993), p. 87.
[17] O. Kahn, *Molecular Magnetism* (VCH Publishers, New York, 1993), p. 380.
[18] T. C. Stamatatos, A. K. Boudalis, V. Sanakis, and Catherine P. Raptopoulou, Inorg. Chem. **45**, 7372 (2006).
[19] A. K. Boudalis, N. Lalioti, G. A. Spyroulias, Th. C. Stamatatos, C. P. Raptopoulou, A. Terzis, A. Bousseksou, V. Tangoulis, J.-P. Tuchagues, and S. P. Perlepes, Inorg. Chem. **41**, 6474 (2002).
[20] A. K. Boudalis, V. Tangoulis, C. P. Raptopoulou, A. Terzis, J.-P. Tuchagues, and S. P. Perlepes, Inorg. Chim. Acta **357**, 1345 (2004).
[21] J. Overgaard, D. E. Hibbs, E. Rentschler, G. A. Timco, and F. K. Larsen, Inorg. Chem. **42**, 7593 (2003).
[22] P. Chauduri, E. Rentschler, F. Birkelbach, C. Krebs, E. Bill, T. Weyhermuller, and U. Flurke, Eur. J. Inorg. Chem. **3**, 541, (2003).
[23] J. K. McCusker, J. B. Vincent, E. A. Schmit, M. L. Mino, J. Shin, D. A. K. Coggin, P. M. Hagen, J. C. Hauffman, G. Christou, and D. N. Hendrickson, J. Am. Chem. Soc. **113**, 3012 (1991).
[24] B. Yan and Z.-D. Chen, Inorg. Chem. Commun. **4**, 138 (2001); K. I. Turte, S. A. Bobkova, B. Kuyavskaya, I. N. Ivleva, V. I. Ponomarev, and M. E. Veksel'man, J. Coord. Chem. **11**, 1106 (1985).
[25] D. Prodius, V. Mereacre, S. Shova, M. Gdaniec, Y. Simonov, L. Sorace, A. Caneschi, N. Stanica, I. Geru, and C. Turta, Chem. J. Moldova **1**, 95 (2006).
[26] C. Cañada-Vilalta, T. A. O'Brian, E. K. Brechin, M. Pink, E. R. Davidson, and G. Christou, Inorg. Chem. **43**, 5505 (2004).
[27] Ref. tables for μ_{eff} of the free Ln(III) ions; www.radiochemistry.org/periodictable/la_series/L8.html
[28] A. Abragam and B. Bleaney, *Electron Paramagnetic Resonance of Transition Ions* (Clarendon Press, Oxford, 1970), p. 316.
[29] F. Luis, J. Bartolomé, J. F. Fernández, J. Tejada, J. M. Hernández, X. X. Zhang, and R. Ziolo, Phys. Rev. B **55**, 11448 (1997).
[30] L. Cianchi, F. Del Giallo, G. Spina, W. Reiff, and A. Caneschi, Phys. Rev. B **65**, 064415 (2002); G. Filoti, J. Bartolome, V. Kuncser, Ioana Mindru, and Luminita Patron, J. Magn. Magn. Mater. **310**, 1452 (2007).
[31] A. K. Boudalis, Y. Sanakis, J. M. Clemente-Juan, A. Mari, and J.-P. Tuchagues, Eur. J. Inorg. Chem. **2007**, 2409.
[32] M. F. Thomas and C. E. Johnson, in *Mössbauer Spectroscopy*, edited by D. P. E. Dickinson and F. J. Berry (Cambridge University Press, Cambridge, 1986).
[33] J. van Slageren, P. Rosa, A. Caneschi, R. Sessoli, H. Casellas, Y. V. Rakitin, L. Cianchi, F. del Giallo, G. Spina, A. Bino, A.-L. Barra, T. Guidi, S. Carretta, and R. Caciuffo, Phys. Rev. B **73**, 014422 (2006).
[34] R. V. Pound and G. A. Rebka, Phys. Rev. Lett. **4**, 274 (1960); B. D. Josephson, *ibid.* **4**, 341 (1960).
[35] V. I. Ponomarev, L. O. Atovmyan, S. A. Bobkova, and K. I. Turte, Dokl. Akad. Nauk SSSR **274**, 368 (1984); R. A. Stukan, V. I. Ponomarev, V. P. Nifontov, K. I. Turte, and L. O. Atovmyan, J. Struct. Chem. **26**, 197 (1985).
[36] W. H. Armstrong, M. E. Roth, and S. J. Lippard, J. Am. Chem. Soc. **109**, 6318 (1987).
[37] T. Glaser and T. Lugger, Inorg. Chim. Acta **337**, 103 (2002).
[38] J. H. Satcher, Jr., M. M. Olmstead, M. W. Droege, S. R. Parkin, B. C. Noll, L. May, and A. L. Balch, Inorg. Chem. **37**, 6751 (1998).
[39] S. M. Gorun and S. J. Lippard, Inorg. Chem. **27**, 149 (1988).
[40] M. W. Wemple, D. A. K. Coggin, J. B. Vincent, J. K. McCusker, W. E. Streib, J. C. Huffman, D. N. Hendrickson, and G. J. Christou, J. Chem. Soc. Dalton Trans. **1998**, 719.
[41] T. Sato, F. Ambe, K. Endo, M. Katada, H. Maeda, T. Nakamoto, and H. Sano, J. Am. Chem. Soc. **118**, 3450 (1996).
[42] S. K. Abdulaev, O. A. Nasonova, K. I. Yakubov, K. I. Turte, V. V. Zelentsov, and R. A. Stukan, Zh. Neorg. Khim. **33**, 1765 (1988).